

# A Volume Temperature Relationship for Liquid GeO<sub>2</sub> and some Geophysically Relevant Derived Parameters for Network Liquids

D.B. Dingwell, R. Knoche, and S.L. Webb

Bayerisches Geoinstitut, Universität Bayreuth, Postfach 101251, W-8580 Bayreuth, Federal Republic of Germany

Received June 10, 1992 / Revised, accepted October 17, 1992

**Abstract.** The thermal expansivity of liquid GeO<sub>2</sub> at temperatures just above the glass transition has been obtained using a combination of scanning calorimetry and dilatometry. The calorimetric and dilatometric curves of  $c_p$  and  $dV/dT$  are normalized to the temperature derivative of fictive temperature versus temperature using the method of Webb et al. (1992). This normalization, based on the equivalence of relaxation parameters for volume and enthalpy, allows the completion of the dilatometric trace across the glass transition to yield liquid expansivity and volume. The values of liquid volume and expansivity obtained in this study are combined with high temperature densitometry determinations of the liquid volume of GeO<sub>2</sub> by Sekiya et al. (1980) to yield a temperature-volume relation for GeO<sub>2</sub> melt from 660 to 1400 °C. Liquid GeO<sub>2</sub> shows a strongly temperature-dependent liquid molar expansivity, decreasing from  $20.27 \times 10^{-4} \text{ cm}^3 \text{ mol}^{-1} \text{ }^\circ\text{C}^{-1}$  to  $1.97 \times 10^{-4} \text{ cm}^3 \text{ mol}^{-1} \text{ }^\circ\text{C}^{-1}$  with increasing temperature. The coefficient of volume thermal expansion ( $\alpha_v$ ) decreases from  $76.33 \times 10^{-6} \text{ }^\circ\text{C}^{-1}$  to  $2.46 \times 10^{-6} \text{ }^\circ\text{C}^{-1}$  with increasing temperature. A qualitatively similar volume-temperature relationship, with  $\alpha_v$  decreasing from  $335 \times 10^{-6} \text{ }^\circ\text{C}^{-1}$  to  $33 \times 10^{-6} \text{ }^\circ\text{C}^{-1}$  with increasing temperature, has been observed previously in liquid B<sub>2</sub>O<sub>3</sub>. The determination of the glass transition temperature, liquid volume, liquid and glassy expansivities and heat capacities in this study, combined with compressibility data for glassy and liquid GeO<sub>2</sub> from the literature (Soga 1969; Kurkjian et al. 1972; Scarfe et al. 1987) allows the calculation of the Prigogine-Defay ratio ( $\Pi$ ),  $c_p - c_v$  and the thermal Grüneisen parameter ( $\gamma_{\text{th}}$ ) for GeO<sub>2</sub>. From available data on liquid SiO<sub>2</sub> it is concluded that liquid GeO<sub>2</sub> is not a good analog for the low pressure properties of liquid SiO<sub>2</sub>.

## Introduction

GeO<sub>2</sub> is commonly used as an analog of SiO<sub>2</sub> in studies of the structure and properties of glasses, liquids (Richet 1990) and minerals (Ross et al. 1986; Rigden and Jack-

son 1991). The isomorphous nature of amorphous GeO<sub>2</sub> and SiO<sub>2</sub> has been emphasized in spectroscopic studies (e.g. Konnert et al. 1973). Glassy GeO<sub>2</sub> investigated at high pressure has been shown to undergo a coordination shift (Durben and Wolf 1991; Itie et al. 1989) and the addition of alkalis to GeO<sub>2</sub> glass and liquid also produces a density and bulk modulus maximum that has been interpreted as resulting from a shift to higher coordination (Riebling 1963; Sekiya et al. 1980; Osaka et al. 1985; see, however, Henderson and Fleet 1991). For studies of the liquid state, GeO<sub>2</sub> provides the considerable advantage that the temperature required to achieve the relaxed liquid response of amorphous GeO<sub>2</sub> is 500–600 °C lower than that of SiO<sub>2</sub>, at any given frequency. The lower temperature of structural relaxation in GeO<sub>2</sub> (at approx. 580 °C versus 1180 °C for SiO<sub>2</sub> at approx.  $10^{-2}$  Hz) brings studies of the glass transition of this single component network-structure liquid within the temperature range of operation of very precise scanning methods of dilatometry and calorimetry.

In a recent series of studies, the analysis of scanning calorimetric and dilatometric data across the glass transition of silicate melts has been used to obtain liquid thermal expansivity data just above glass transition temperatures (Knoche et al. 1992a, b, c). These low-temperature liquid expansivities have been combined with high temperature densitometry to obtain the first reliable estimates of the temperature-dependence of thermal expansivity in silicate melts. By using these methods, we present an expression for the volume-temperature relationship of GeO<sub>2</sub> liquid from 660 to 1400 °C. The volume and expansivity data point in a consistent manner to a strongly temperature-dependent expansivity for liquid GeO<sub>2</sub>.

The new data on the changes in heat capacity and thermal expansivity across the glass transition, the molar volume at the glass transition and the glass transition temperature are combined with literature-derived estimates of the compressibility of GeO<sub>2</sub> glass and liquid to estimate the values of the Prigogine-Defay ratio,  $c_p - c_v$  and the thermal Grüneisen parameter for amor-

**Table 1.** Measured  $c_p$  ( $J g^{-1} °C^{-1}$ ) data for glass and liquid  $GeO_2$ . (heating-rate  $5 °C min^{-1}$ )

| $T(°C)$ | Cooling rate    |                 |                 |                  |
|---------|-----------------|-----------------|-----------------|------------------|
|         | $1 °C min^{-1}$ | $2 °C min^{-1}$ | $5 °C min^{-1}$ | $10 °C min^{-1}$ |
| 40      | 0.5257          | 0.5232          | 0.5228          | 0.5264           |
| 50      | 0.5330          | 0.5313          | 0.5299          | 0.5348           |
| 60      | 0.5356          | 0.5342          | 0.5325          | 0.5382           |
| 70      | 0.5463          | 0.5454          | 0.5433          | 0.5489           |
| 80      | 0.5523          | 0.5536          | 0.5505          | 0.5561           |
| 90      | 0.5592          | 0.5614          | 0.5557          | 0.5615           |
| 100     | 0.5647          | 0.5671          | 0.5595          | 0.5668           |
| 110     | 0.5702          | 0.5731          | 0.5640          | 0.5727           |
| 120     | 0.5758          | 0.5792          | 0.5689          | 0.5786           |
| 130     | 0.5808          | 0.5848          | 0.5743          | 0.5840           |
| 140     | 0.5856          | 0.5900          | 0.5791          | 0.5891           |
| 150     | 0.5905          | 0.5951          | 0.5833          | 0.5940           |
| 160     | 0.5952          | 0.6001          | 0.5876          | 0.5988           |
| 170     | 0.5997          | 0.6044          | 0.5913          | 0.6031           |
| 180     | 0.6045          | 0.6091          | 0.5979          | 0.6078           |
| 190     | 0.6091          | 0.6138          | 0.6033          | 0.6122           |
| 200     | 0.6131          | 0.6176          | 0.6074          | 0.6162           |
| 210     | 0.6164          | 0.6209          | 0.6111          | 0.6194           |
| 220     | 0.6197          | 0.6241          | 0.6146          | 0.6226           |
| 230     | 0.6228          | 0.6268          | 0.6178          | 0.6256           |
| 240     | 0.6258          | 0.6290          | 0.6207          | 0.6284           |
| 250     | 0.6286          | 0.6309          | 0.6236          | 0.6309           |
| 260     | 0.6317          | 0.6329          | 0.6263          | 0.6335           |
| 270     | 0.6348          | 0.6347          | 0.6289          | 0.6354           |
| 280     | 0.6377          | 0.6370          | 0.6312          | 0.6377           |
| 290     | 0.6415          | 0.6404          | 0.6337          | 0.6409           |
| 300     | 0.6447          | 0.6438          | 0.6370          | 0.6443           |
| 310     | 0.6483          | 0.6480          | 0.6411          | 0.6487           |
| 320     | 0.6513          | 0.6511          | 0.6446          | 0.6516           |
| 330     | 0.6532          | 0.6511          | 0.6471          | 0.6536           |
| 340     | 0.6540          | 0.6488          | 0.6479          | 0.6543           |
| 350     | 0.6546          | 0.6501          | 0.6475          | 0.6545           |
| 360     | 0.6572          | 0.6503          | 0.6481          | 0.6552           |
| 370     | 0.6583          | 0.6510          | 0.6502          | 0.6570           |
| 380     | 0.6594          | 0.6534          | 0.6523          | 0.6590           |
| 390     | 0.6605          | 0.6554          | 0.6540          | 0.6601           |
| 400     | 0.6614          | 0.6571          | 0.6551          | 0.6614           |
| 410     | 0.6623          | 0.6584          | 0.6555          | 0.6615           |
| 420     | 0.6636          | 0.6603          | 0.6564          | 0.6626           |
| 430     | 0.6648          | 0.6613          | 0.6578          | 0.6645           |
| 440     | 0.6662          | 0.6628          | 0.6592          | 0.6653           |
| 450     | 0.6669          | 0.6640          | 0.6602          | 0.6654           |
| 460     | 0.6677          | 0.6649          | 0.6610          | 0.6658           |
| 470     | 0.6689          | 0.6663          | 0.6623          | 0.6664           |
| 480     | 0.6695          | 0.6677          | 0.6634          | 0.6662           |
| 490     | 0.6708          | 0.6690          | 0.6640          | 0.6662           |
| 500     | 0.6730          | 0.6711          | 0.6653          | 0.6668           |
| 510     | 0.6764          | 0.6745          | 0.6676          | 0.6685           |
| 520     | 0.6810          | 0.6786          | 0.6704          | 0.6711           |
| 530     | 0.6885          | 0.6848          | 0.6756          | 0.6757           |
| 540     | 0.6999          | 0.6944          | 0.6831          | 0.6836           |
| 550     | 0.7148          | 0.7079          | 0.6938          | 0.6946           |
| 560     | 0.7323          | 0.7246          | 0.7081          | 0.7088           |
| 570     | 0.7475          | 0.7399          | 0.7242          | 0.7240           |
| 580     | 0.7541          | 0.7475          | 0.7359          | 0.7343           |
| 590     | 0.7523          | 0.7463          | 0.7390          | 0.7383           |
| 600     | 0.7441          | 0.7403          | 0.7358          | 0.7373           |
| 610     | 0.7357          | 0.7339          | 0.7299          | 0.7339           |
| 620     | 0.7313          | 0.7309          | 0.7255          | 0.7313           |
| 630     | 0.7298          | 0.7299          | 0.7239          | 0.7301           |
| 640     | 0.7293          | 0.7296          | 0.7228          | 0.7293           |
| 650     | 0.7292          | 0.7297          | 0.7217          | 0.7291           |
| 660     | 0.7288          | 0.7294          | 0.7210          | 0.7287           |

**Table 1** (continued)

| $T(°C)$          | Cooling rate    |                 |                 |                  |
|------------------|-----------------|-----------------|-----------------|------------------|
|                  | $1 °C min^{-1}$ | $2 °C min^{-1}$ | $5 °C min^{-1}$ | $10 °C min^{-1}$ |
| 670              | 0.7287          | 0.7295          | 0.7204          | 0.7285           |
| 680              | 0.7281          | 0.7292          | 0.7195          | 0.7276           |
| 690              | 0.7273          | 0.7285          | 0.7191          | 0.7270           |
| Peak temperature | 578 °C          | 578 °C          | 584 °C          | 583 °C           |

Note: The heat capacities are estimated to have a precision of  $\pm 1\%$ ;  $T_g$  = peak temperature

phous and liquid  $GeO_2$ . Using existing data for  $SiO_2$ , comparisons are made with the volume-temperature relation and derived parameters.

### Calorimetry and Dilatometry

The sample of  $GeO_2$  glass used in the present investigation was made by direct fusion of  $GeO_2$  (ultrapure, Alfa<sup>®</sup>) powder in a platinum crucible in a vertical tube furnace operating in air at  $1400 °C$ . The sample was stirred with a  $Pt_{80}Rh_{20}$  rod for several hours to promote fining. After sufficient time for fining, the spindle was removed from the sample, and the crucible was removed from the furnace to cool in air. A 6.4 mm diameter cylinder was bored from the cooled sample with a diamond coring tool and this cylinder was cut to a length of 1 cm using a diamond saw. The cylinder was stored in a desiccator until use in the dilatometer and calorimeter.

The calorimetry was performed in continuous scanning mode with a Setaram<sup>®</sup> DSC instrument. The heat flow was recorded during heating runs of  $5 °C min^{-1}$  on glasses that had been previously cooled from  $\sim 100 °C$  above  $T_g$  (see Table 1) at cooling rates of 1, 2, 5 and  $10 °C min^{-1}$ . The calorimeter was calibrated regularly against a geometrically identical cylinder of sapphire, using the heat capacity data of Robie et al. (1979). The heat capacity data are presented in Table 1. The heat capacities are estimated to have a precision of  $\pm 1\%$  at  $1\sigma$ , based on the 4 runs performed for each sample. The measured heat capacities are in excellent agreement with those reported in Robie et al. (1979), but 3% lower than the more recent data of Richet (1990). The reasons for this discrepancy are not clear. A typical calorimetric trace, that obtained for  $1 °C min^{-1}/5 °C min^{-1}$  (cooling-rate/heating-rate) is illustrated in Fig. 1a.

The dilatometry was performed with a Netzsch<sup>®</sup> TMA 402 quartz-rod dilatometer. The sample, its thermal history and the scanning rates were those used in the calorimetry measurements. This instrument has been calibrated against single crystal sapphire (NBS sheet 732). The molar expansivity of the glass has an accuracy of  $\pm 3\%$  at  $1\sigma$ , calculated from the errors in

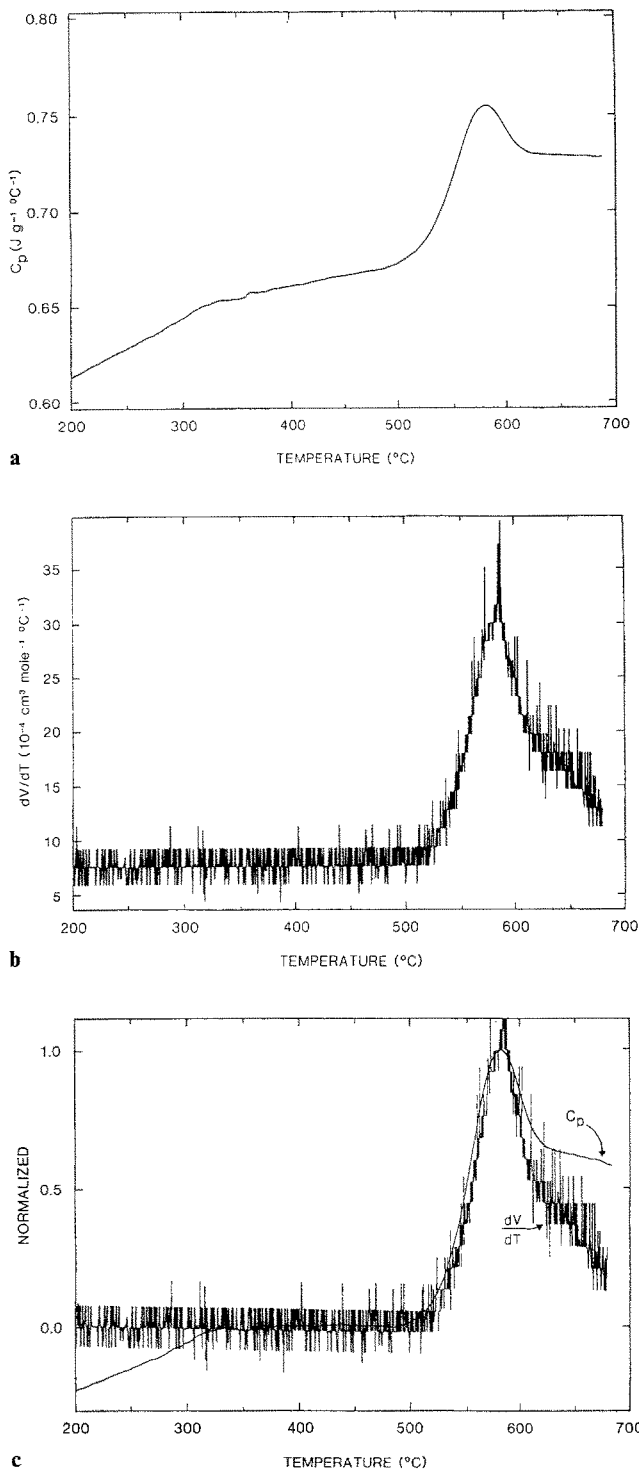


**Fig. 1.** Calorimetric **a** and dilatometric **b** traces of the glass transition for amorphous  $\text{GeO}_2$  **c** normalized comparison of heat capacity and expansivity for liquid  $\text{GeO}_2$ . ( $1^\circ\text{C min}^{-1}$  cooling rate/ $5^\circ\text{C min}^{-1}$  heating rate)

the measurements of the thermal expansivity of the standard ( $\pm 2\%$ ) and the sample ( $\pm 2\%$ ). The room temperature density of the glass [ $\rho(15.5^\circ\text{C}) = 3.651 \pm 0.004 \text{ g cm}^{-3}$ ] was determined by Archimedean densitometry in toluene. The molar thermal expansion data calculated from the room temperature volume

[ $V(15.5^\circ\text{C}) = 28.65 \pm 0.03 \text{ cm}^3 \text{ mol}^{-1}$ ] combined with the dilatometric data for the glass, are presented in Table 2. The dilatometry trace for  $\text{GeO}_2$  ( $1^\circ\text{C min}^{-1}/5^\circ\text{C min}^{-1}$ ) is illustrated in Fig. 1 b.

### Derivation of Liquid Expansivity

The derivation of liquid expansivity and volume from calorimetric and dilatometric data is based on the principles of structural relaxation in silicate melts (Narayanaswamy 1971; Moynihan et al. 1976; Scherer 1984). The more general aspects of structural relaxation in silicate melts, their influence on diffusion, viscosity, heat capacity and density, have been discussed previously (e.g. Richet and Bottinga 1986; Dingwell 1990; Dingwell and Webb 1989, 1990). The theory of our procedure for obtaining relaxed liquid molar expansivity data from a combination of scanning calorimetry and dilatometry has been presented in full by Webb et al. (1992). This method of determining the volume and thermal expansivity of relaxed supercooled melts has been successfully tested against the volume and thermal expansivity extrapolated from high temperature double-bob Archimedean density measurements in silicate melts (Knoche et al. 1992 a, b, c).

The physical properties of a silicate melt depend upon the configuration or structure of the melt and the ambient temperature  $T$ . The configuration of silicate glasses quenched from liquids can be approximated to the equilibrium structure of the liquid at some fictive temperature,  $T_f$ . The temperature-derivatives of glass properties can be used to describe the temperature-derivative of the fictive temperature. To do this, the temperature-derivative of any property in the glass transition interval is normalized with respect to the temperature-derivative of the liquid and glassy properties. The temperature-derivative of the fictive temperature  $T_f$  at a temperature  $T'$  is related to the temperature dependence of a macroscopic property  $\Phi$  by;

$$\left. \frac{dT_f}{dT} \right|_{T'} = \frac{[(\partial \Phi / \partial T) - (\partial \Phi / \partial T)_g]_{T'}}{[(\partial \Phi / \partial T)_e - (\partial \Phi / \partial T)_g]_{T'}} \quad (1)$$

where the subscripts “e” and “g” are for the liquid (equilibrium) and the glassy values of the property (Moynihan et al. 1976). In order to describe the physical properties of a melt in the glass transition region it is necessary to devise an algorithm for the temperature dependence of the fictive temperature.

In the present study, enthalpy  $H$ , and volume  $V$  take the place of the general property  $\Phi$  in [1]. Assuming the equivalence of volume and enthalpy relaxation behavior in the glass transition region (c.f., Webb 1992), Equation 1 can then be rewritten as;

$$\frac{c_p(T') - c_{pg}(T')}{c_{pe}(T_f) - c_{pg}(T_f)} = \left. \frac{dT_f}{dT} \right|_{T'} = \frac{\left[ \frac{dV(T)}{dT} - \frac{dV_g(T)}{dT} \right]_{T'}}{\left[ \frac{dV_e(T)}{dT} - \frac{dV_g(T)}{dT} \right]_{T'}} \quad (2)$$

**Table 2.** Measured  $dV/dT(10^{-4} \text{ cm}^3 \text{ mol}^{-1} \text{ }^\circ\text{C}^{-1})$  data for glass and liquid  $\text{GeO}_2$ . (heating-rate  $5 \text{ }^\circ\text{C min}^{-1}$ )

| $T(^\circ\text{C})$ | Cooling rate                        |                                     |                                     |                                      |
|---------------------|-------------------------------------|-------------------------------------|-------------------------------------|--------------------------------------|
|                     | $1 \text{ }^\circ\text{C min}^{-1}$ | $2 \text{ }^\circ\text{C min}^{-1}$ | $5 \text{ }^\circ\text{C min}^{-1}$ | $10 \text{ }^\circ\text{C min}^{-1}$ |
| 40                  | 4.18                                | 5.31                                | 5.33                                | 4.95                                 |
| 50                  | 6.15                                | 6.62                                | 6.53                                | 5.46                                 |
| 60                  | 7.40                                | 7.27                                | 5.64                                | 7.21                                 |
| 70                  | 7.08                                | 7.39                                | 7.18                                | 6.92                                 |
| 80                  | 7.20                                | 7.40                                | 6.61                                | 7.67                                 |
| 90                  | 7.32                                | 7.30                                | 7.10                                | 7.10                                 |
| 100                 | 7.32                                | 7.32                                | 6.45                                | 7.20                                 |
| 110                 | 7.21                                | 7.10                                | 7.54                                | 6.72                                 |
| 120                 | 7.61                                | 7.20                                | 7.88                                | 7.51                                 |
| 130                 | 7.35                                | 6.78                                | 8.14                                | 7.45                                 |
| 140                 | 7.27                                | 7.35                                | 7.84                                | 7.11                                 |
| 150                 | 7.19                                | 7.29                                | 7.20                                | 7.27                                 |
| 160                 | 7.21                                | 7.63                                | 7.49                                | 7.50                                 |
| 170                 | 7.78                                | 7.34                                | 7.75                                | 7.46                                 |
| 180                 | 7.74                                | 7.89                                | 8.58                                | 7.48                                 |
| 190                 | 8.04                                | 8.09                                | 6.98                                | 7.92                                 |
| 200                 | 7.93                                | 8.09                                | 7.69                                | 7.91                                 |
| 210                 | 7.44                                | 7.28                                | 8.30                                | 7.60                                 |
| 220                 | 7.61                                | 7.36                                | 7.93                                | 6.91                                 |
| 230                 | 7.73                                | 7.46                                | 7.20                                | 6.39                                 |
| 240                 | 7.58                                | 7.66                                | 7.89                                | 8.41                                 |
| 250                 | 7.20                                | 7.80                                | 6.49                                | 5.84                                 |
| 260                 | 7.50                                | 8.05                                | 7.50                                | 7.45                                 |
| 270                 | 7.78                                | 8.10                                | 7.90                                | 7.68                                 |
| 280                 | 7.78                                | 8.33                                | 8.36                                | 8.10                                 |
| 290                 | 8.04                                | 8.02                                | 7.98                                | 7.24                                 |
| 300                 | 7.86                                | 8.31                                | 7.05                                | 7.11                                 |
| 310                 | 7.86                                | 7.69                                | 8.45                                | 7.62                                 |
| 320                 | 7.77                                | 7.46                                | 8.27                                | 8.75                                 |
| 330                 | 7.99                                | 8.03                                | 6.48                                | 7.13                                 |
| 340                 | 7.95                                | 7.68                                | 7.19                                | 7.50                                 |
| 350                 | 7.67                                | 7.84                                | 7.71                                | 7.37                                 |
| 360                 | 7.98                                | 7.38                                | 6.73                                | 7.29                                 |
| 370                 | 7.81                                | 7.51                                | 7.05                                | 8.20                                 |
| 380                 | 7.69                                | 7.69                                | 7.70                                | 6.96                                 |
| 390                 | 7.61                                | 7.49                                | 8.64                                | 7.66                                 |
| 400                 | 8.55                                | 7.96                                | 7.18                                | 7.59                                 |
| 410                 | 7.88                                | 7.67                                | 7.25                                | 7.55                                 |
| 420                 | 8.00                                | 7.63                                | 7.68                                | 7.17                                 |
| 430                 | 7.47                                | 7.47                                | 7.69                                | 8.20                                 |
| 440                 | 7.90                                | 7.48                                | 7.71                                | 6.66                                 |
| 450                 | 7.97                                | 7.56                                | 7.73                                | 7.86                                 |
| 460                 | 7.94                                | 7.81                                | 7.27                                | 6.66                                 |
| 470                 | 8.29                                | 7.89                                | 7.89                                | 6.50                                 |
| 480                 | 7.97                                | 8.14                                | 8.62                                | 7.26                                 |
| 490                 | 8.42                                | 8.38                                | 5.44                                | 7.00                                 |
| 500                 | 8.10                                | 8.14                                | 5.29                                | 6.58                                 |
| 510                 | 8.73                                | 8.41                                | 7.34                                | 6.70                                 |
| 520                 | 9.57                                | 9.08                                | 7.26                                | 8.91                                 |
| 530                 | 10.68                               | 10.30                               | 8.58                                | 6.69                                 |
| 540                 | 13.01                               | 11.64                               | 10.05                               | 9.24                                 |
| 550                 | 16.68                               | 14.37                               | 12.52                               | 12.44                                |
| 560                 | 21.43                               | 19.26                               | 14.88                               | 15.53                                |
| 570                 | 26.47                               | 24.22                               | 19.71                               | 20.57                                |
| 580                 | 30.06                               | 28.07                               | 23.79                               | 22.19                                |
| 590                 | 29.97                               | 28.13                               | 26.28                               | 24.38                                |
| 600                 | 24.62                               | 24.25                               | 22.70                               | 24.24                                |
| 610                 | 20.82                               | 20.57                               | 19.65                               | 20.48                                |
| 620                 | 19.07                               | 19.07                               | 17.53                               | 20.16                                |
| 630                 | 17.75                               | 18.97                               | 16.81                               | 18.42                                |
| 640                 | 17.44                               | 18.61                               | 15.01                               | 16.64                                |
| 650                 | 16.09                               | 15.68                               | 13.31                               | 12.30                                |
| 660                 | 15.27                               | 14.78                               | 11.03                               | 11.10                                |

**Table 2** (continued)

| $T(^\circ\text{C})$ | Cooling rate                        |                                     |                                     |                                      |
|---------------------|-------------------------------------|-------------------------------------|-------------------------------------|--------------------------------------|
|                     | $1 \text{ }^\circ\text{C min}^{-1}$ | $2 \text{ }^\circ\text{C min}^{-1}$ | $5 \text{ }^\circ\text{C min}^{-1}$ | $10 \text{ }^\circ\text{C min}^{-1}$ |
| 670                 | 13.86                               | 13.94                               | 8.00                                | 9.33                                 |
| 680                 | 6.63                                | 6.57                                | 3.68                                | 4.75                                 |
| Peak temperature    | 583 $^\circ\text{C}$                | 585 $^\circ\text{C}$                | 588 $^\circ\text{C}$                | 586 $^\circ\text{C}$                 |

Note: The thermal expansion is estimated to have a precision of  $\pm 3\%$

In the above equation relating  $c_p$  and thermal expansivity  $dV/dT$  in the glass transition region, the only unknown parameter is the thermal expansivity of the relaxed liquid at temperature  $T'$  above the glass transition temperature. Despite a common origin, various melt properties can, theoretically differ in relaxation behavior. This would imply different relaxation kinetics due to different partitioning of volume and enthalpy amongst the distribution of structures in the melt. Often, however, no such difference can be distinguished (e.g. Rekhson et al. 1971; Sasabe et al. 1977) and the assumption of equivalent relaxation times for different properties can be usefully employed.

Due to the lack of relaxed thermal expansivity data, we recover the liquid molar thermal expansivity from the dilatometric trace by normalizing both the scanning calorimetric and dilatometric data;

$$\Phi'(T) = \frac{\Phi(T) - \Phi_g(T)}{\Phi_p - \Phi_g(T)} \quad (3)$$

where the subscripts "p" and "g" refer to peak and glassy values. The relaxed value of thermal expansivity ( $dV/dT$  at  $T=T'$ ) can now be generated from the peak and linearly extrapolated glassy values of normalized heat capacity and thermal expansion curves (see Fig. 1c and [2]). The volume,  $V$ , and coefficient of volume thermal expansion  $\alpha_v [1/V \cdot (dV/dT)]$  of the melt at  $T=T'$  can also be calculated. It should be emphasized that the above method can only be applied to calorimetric and dilatometric data obtained on the same sample using identical experimental conditions and thermal histories. It is only this internal consistency that permits the use of the assumption of the equivalence of the enthalpy and volume relaxation behavior as small changes in composition or fictive temperature of the melt can strongly influence relaxation behavior.

The volume and expansivity of liquid  $\text{GeO}_2$  at the glass transition may be compared with liquid  $\text{GeO}_2$  density data obtained by Sekiya et al. (1980) using the restrained sphere method. These data at higher temperatures are presented together with our data in Figure 2 and Table 3. The volume-temperature relationship consistent with all the volume data together with the thermal expansion determined at  $T=660 \text{ }^\circ\text{C}$  is best described by

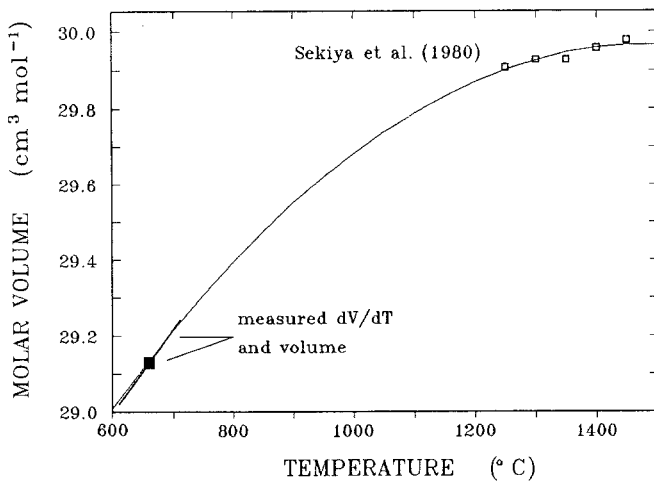


**Fig. 2.** The volume temperature relationship of liquid  $\text{GeO}_2$  from the glass transition to 1400 °C. High temperature data from Sekiya et al. (1980)

**Table 3.** Molar volume of  $\text{GeO}_2$  as a function of temperature. High temperature data from Sekiya et al. (1980)

| Temperature (°C) | Volume ( $\text{cm}^3 \text{mol}^{-1}$ ) |
|------------------|--|
| 660              | 29.1322                                  |
| 1250             | 29.91                                    |
| 1300             | 29.93                                    |
| 1350             | 29.96                                    |
| 1400             | 29.96                                    |
| 1450             | 29.98                                    |

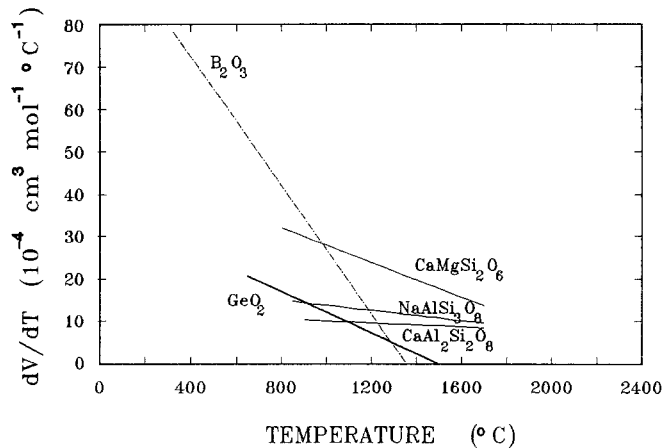


**Fig. 3.** Thermal expansion of  $\text{B}_2\text{O}_3$ ,  $\text{GeO}_2$ ,  $\text{NaAlSi}_3\text{O}_8$ ,  $\text{CaAl}_2\text{Si}_2\text{O}_8$  and  $\text{CaMgSi}_2\text{O}_6$  liquids as a function of temperature

the polynomial;

$$V(\text{cm}^3 \text{mol}^{-1}) = 27.26(0.06) + 3.67(0.14) \times 10^{-3} T - 1.23(0.07) \times 10^{-6} T^2 \quad (4)$$

for temperature in °C. The expansivity obtained from [4] for liquid  $\text{GeO}_2$  at 660 °C ( $20.46 \pm 1.68 \times 10^{-4} \text{cm}^3 \text{mol}^{-1} \text{°C}^{-1}$ ) is within error of that determined using our dilatometry/calorimetry method

( $22.23 \pm 0.96 \times 10^{-4} \text{cm}^3 \text{mol}^{-1} \text{°C}^{-1}$ ). The expansivity of the liquid decreases strongly (an order of magnitude) as temperature increases from 660 to 1400 °C. Qualitatively similar behavior has been observed for liquid  $\text{B}_2\text{O}_3$  (Napolitano et al. 1965) and for a wide range of liquids in the anorthite-albite-diopside system (Knoche et al. 1992a, b), as illustrated in Fig. 3.

### The Prigogine-Defay Ratio (II)

For the case in which a single order parameter, along with temperature and pressure conditions, is sufficient to specify the state of a system, the Prigogine-Defay ratio must be unity. Where this is not the case, the question arises as to how many independent parameters of the structure are needed to describe the relaxation of properties across the glass transition. The Prigogine-Defay ratio  $\Pi$  is given by;

$$\Pi = \frac{\Delta\beta \Delta c_p}{(\Delta\alpha_v)^2 T_g V} \quad (5)$$

where  $T_g$  is the glass transition temperature,  $\Delta\beta$  is the difference between the compressibility of the liquid and the glass at  $T_g$ ,  $\Delta c_p$  is the difference between the heat capacity of the liquid and the glass at  $T_g$ ,  $\Delta\alpha_v$  is the difference between the coefficient of volume thermal expansion of the liquid and the glass at  $T_g$  and  $V$  is the molar volume at  $T_g$  (Lesikar and Moynihan 1980; Gupta and Moynihan 1976; Nemilov et al. 1987).

We can use our data of the glassy and liquid values of heat capacity and expansivity, the glass transition temperature and the volume at this temperature to calculate the Prigogine-Defay ratio for liquid  $\text{GeO}_2$ . The remaining data required are the compressibility of the glass and the liquid. The compressibility of glassy  $\text{GeO}_2$  has been measured at low temperature by Soga (1969) using ultrasonic (20 MHz pulse superposition) methods. The temperature dependence of the glass compressibility has been determined by Kurkjian et al. (1972). The liquid compressibility of  $\text{GeO}_2$  has not been measured at 0.1 MPa but density data for the liquid at 1425° C and pressures of 1, 1.5 and 2 GPa are provided by Scarfe et al. (1987) using the falling sphere method. These high pressure densities combined with the 0.1 MPa, 1400 °C density of  $\text{GeO}_2$  from Sekiya et al. (1980) can be described by the polynomial volume-pressure relationship;

$$V(\text{cm}^3 \text{mol}^{-1}) = 30.019(0.024) - 3.77(0.11) P + 1.86(0.12) P^2 \quad (6)$$

for pressure in GPa.

The 0.1 MPa compressibility [ $\beta = -(1/V) \cdot (dV/dP)$ ] calculated from [6] is  $12.4(0.4) \times 10^{-11} \text{Pa}^{-1}$ . The data used in the calculation of the Prigogine-Defay ratio, their uncertainties and sources are summarized in Table 4. The resultant value of  $\Pi$  is  $6.9 \pm 1.3$ . This value compares favorably with the range of values typical for silicate melts (see Table 4) indicating that the relaxation behavior of a pure network component like  $\text{GeO}_2$  is qualita-

**Table 4.** Data used in the calculation of the derived parameters for GeO<sub>2</sub>

| Property   | T(°C) | liquid                  | glass                   | $\Phi_l - \Phi_g$ |
|--|-------|-------------------------|-------------------------|-------------------|
| K(GPa)   | 660   | 8.08(24) <sup>a,b</sup> | 23.87(3) <sup>c,d</sup> |                   |
|  | 1400  | 8.08                    |                         |                   |
| $\beta(10^{-11} \text{ Pa}^{-1})$                    | 660   | 12.4(4) <sup>a,b</sup>  | 4.19 <sup>c,d</sup>     | 8.19 ± 0.40       |
|  | 1400  | 12.4                    |                         |                   |
| $\alpha_v(10^{-6} \text{ }^\circ\text{C}^{-1})$      | 660   | 76.3(3.3) <sup>f</sup>  | 27.1(7)                 | 49.2 ± 3.4        |
|  | 1400  | 2.46(11) <sup>f</sup>   |                         |                   |
| $c_p(\text{J mol}^{-1} \text{ }^\circ\text{C}^{-1})$ | 660   | 75.9(4) <sup>f</sup>    | 70.4(4)                 | 5.5 ± 0.6         |
|  | 1400  | 80.7 <sup>e</sup>       |                         |                   |
| $V(10^{-6} \text{ m}^3 \text{ mol}^{-1})$            | 660   | 29.13(02) <sup>f</sup>  |                         |                   |
|  | 1400  | 29.96(02) <sup>f</sup>  |                         |                   |

Note: for ease of calculation, the data are presented in SI units

<sup>a</sup> Scarfe et al. 1987

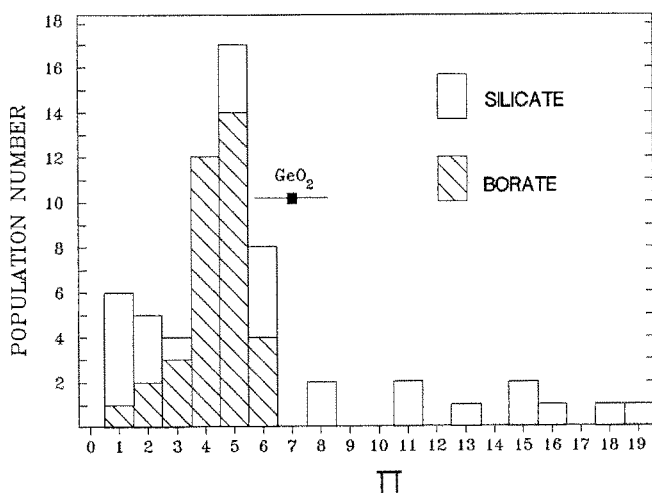
<sup>b</sup> Sekiya et al. 1980

<sup>c</sup> Soga 1969

<sup>d</sup> Kurkjian et al. 1972

<sup>e</sup> Richet et al. 1982

<sup>f</sup> this study

**Fig. 4.** The Prigogine-Defay ratio for silicate and borate glasses compared with that for GeO<sub>2</sub>

tively equivalent to that of more complex silicate and non-silicate compositions. In Fig. 4 we present a histogram of the values of  $\Pi$  that have been derived from literature sources by Nemilov et al. (1987), our value for GeO<sub>2</sub> lies well within the range of values for alkali silicate and borate glasses. Recent data for the ternary system albite-anorthite-diopside (Table 5) result in the determination of  $5 < \Pi < 19$  (see Table 6). The  $\Pi$  calculated for B<sub>2</sub>O<sub>3</sub> using the data presented in Table 7 is 3.6. Gupta and Moynihan (1976) calculated a  $\Pi$  of 4.7 for B<sub>2</sub>O<sub>3</sub> from their data compilation. These two values of  $\Pi$  calculated for B<sub>2</sub>O<sub>3</sub> melt are an indication of the range of values of the Prigogine-Defay ratio which can be obtained using different source data. In view of the errors inherent in the calculation of the Prigogine-Defay ratio, a value  $1 < \Pi < 10$  cannot, at present, be distinguished from 1.

**Table 5.** Data used in the calculation of the derived parameters for albite, anorthite and diopside

| Property   | T(°C) | liquid             | glass              | $\Phi_l - \Phi_g$ |
|--|-------|--------------------|--------------------|-------------------|
| K(GPa)   | $T_g$ | 15–25 <sup>e</sup> | 30–50 <sup>c</sup> |                   |
|  | 1400  | 15–25 <sup>e</sup> |                    |                   |
| $\beta(10^{-11} \text{ Pa}^{-1})$                    | $T_g$ | 4–7                | 2–3                | 1–5               |
|  | 1400  | 4–7                |                    |                   |
| $\alpha_v(10^{-6} \text{ }^\circ\text{C}^{-1})$      | 705   | 54 <sup>a,b</sup>  | 23 <sup>a,b</sup>  | 31                |
|  | 1400  | 3 <sup>a,b</sup>   |                    |                   |
| Anorthite  | 868   | 52 <sup>a,b</sup>  | 19 <sup>a,b</sup>  | 33                |
|  | 1400  | 22 <sup>a,b</sup>  |                    |                   |
| Diopside   | 732   | 125 <sup>a,b</sup> | 35 <sup>a,b</sup>  | 90                |
|  | 1400  | 47 <sup>a,b</sup>  |                    |                   |
| $c_p(\text{J mol}^{-1} \text{ }^\circ\text{C}^{-1})$ | 705   | 332 <sup>a,b</sup> | 300 <sup>a,b</sup> | 32                |
|  | 1400  | 372 <sup>f</sup>   |                    |                   |
| Anorthite  | 868   | 417 <sup>a,b</sup> | 317 <sup>a,b</sup> | 100               |
|  | 1400  | 435 <sup>d</sup>   |                    |                   |
| Diopside   | 732   | 364 <sup>a,b</sup> | 238 <sup>a,b</sup> | 126               |
|  | 1400  | 335 <sup>d</sup>   |                    |                   |
| $V(10^{-6} \text{ m}^3 \text{ mol}^{-1})$            | 705   | 111 <sup>a,b</sup> |                    |                   |
|  | 1400  | 114 <sup>a,b</sup> |                    |                   |
| Anorthite  | 868   | 105 <sup>a,b</sup> |                    |                   |
|  | 1400  | 107 <sup>a,b</sup> |                    |                   |
| Diopside   | 732   | 78 <sup>a,b</sup>  |                    |                   |
|  | 1400  | 82 <sup>a,b</sup>  |                    |                   |

Note: for ease of calculation, the data are presented in SI units

<sup>a</sup> Knoche et al. 1992a

<sup>b</sup> Knoche et al. 1992b

<sup>c</sup> Bansal and Doremus 1986

<sup>d</sup> Richet and Bottinga 1986

<sup>e</sup> Rivers and Carmichael 1987

<sup>f</sup> Richet et al. 1982

**Table 6.** Prigogine-Defay ratio and Grüneisen parameters for the glasses and liquids

|                               | $\Pi$       | $\gamma_{th}(T_g)$ | $\gamma_{th}(T_g)$ | $\gamma_{th}(1400 \text{ }^\circ\text{C})$ |
|-------------------------------|-------------|--------------------|--------------------|--|
| Albite                        | 7.7(3–15)   | 0.26–0.43          | 0.27–0.45          | 0.26–0.43                                  |
| Anorthite                     | 19(7–38)    | 0.19–0.31          | 0.20–0.33          | 0.08–0.14                                  |
| Diopside                      | 5.0(2–10)   | 0.34–0.57          | 0.40–0.67          | 0.17–0.29                                  |
| GeO <sub>2</sub>              | 6.85 ± 1.26 | 0.27 ± 0.04        | 0.24 ± 0.05        | 0.007 ± 0.001                              |
| B <sub>2</sub> O <sub>3</sub> | 3.6         | 0.28               | 0.20               | 0.02                                       |

### The Thermal Grüneisen Parameter ( $\gamma_{th}$ )

The thermal Grüneisen parameter,  $\gamma_{th}$ , is given by

$$\gamma_{th} = \frac{\alpha_v K_s V}{c_p} \quad (7)$$

(Anderson 1989) for  $\alpha_v$ , the coefficient of volume thermal expansion,  $K_s$ , the adiabatic bulk modulus,  $V$ , the molar volume,  $c_p$ , the heat capacity at constant pressure. The thermal Grüneisen parameter is a representation of the thermal energy of a material. It is a measure of the change in pressure on heating at a constant volume. A

**Table 7.** Data used in the calculation of the derived parameters for B<sub>2</sub>O<sub>3</sub>

| Property   | T(°C) | liquid                                | glass                               | $\Phi_l - \Phi_g$      |
|--|-------|---------------------------------------|-------------------------------------|------------------------|
| K(GPa)   | 307   | ~2 <sup>a</sup> [2.5] <sup>f</sup>    | ~11 <sup>b</sup> [8.3] <sup>f</sup> |                        |
|  | 1400  | ~2                                    |                                     |                        |
| $\beta(10^{-11} \text{ Pa}^{-1})$                    | 307   | 5 [40]                                | 9.1 [12] <sup>f</sup>               | 41 [28] <sup>f</sup>   |
|  | 1400  | 5                                     |                                     |                        |
| $\alpha_v(10^{-6} \text{ }^\circ\text{C}^{-1})$      | 307   | 335 <sup>c</sup> [400] <sup>f</sup>   | 57.9 <sup>c</sup> [50] <sup>f</sup> | 277 [350] <sup>f</sup> |
|  | 1400  | 33.4 <sup>c</sup>                     |                                     |                        |
| $c_p(\text{J mol}^{-1} \text{ }^\circ\text{C}^{-1})$ | 307   | 136 <sup>d</sup> [134] <sup>f</sup>   | 89 <sup>d</sup> [91] <sup>f</sup>   | 47 [43] <sup>f</sup>   |
|  | 1400  | 147 <sup>d</sup>                      |                                     |                        |
| $V(10^{-6} \text{ m}^3 \text{ mol}^{-1})$            | 307   | 41.0 <sup>e</sup> [38.8] <sup>f</sup> | 39.2 <sup>e</sup>                   |                        |
|  | 1400  | 46.5 <sup>e</sup>                     |                                     |                        |

Note: for ease of calculation, the data are presented in SI units

<sup>a</sup> Macedo and Litovitz 1965

<sup>b</sup> Capps et al. 1966

<sup>c</sup> Napolitano et al. 1965

<sup>d</sup> Moynihan et al. 1976

<sup>e</sup> Macedo et al. 1966

[<sup>f</sup>] data of Gupta and Moynihan 1976

$\gamma_{th}$  of 0.5–2.8 is observed for crystalline materials (Anderson 1989) and liquids (Boehler and Ramakrishnan 1980) [ $\gamma_{th}$  for water is ~0.1], with  $0.8 < \gamma_{th} < 1.4$  being assumed for the Earth (Stacey 1977). For silicate melts, a  $\gamma_{th}$  of 0.1–0.4 is observed (see Table 6). Below their respective glass transition temperatures,  $0.19 < \gamma_{th} < 0.57$  for albite, diopside and anorthite composition glasses. Above the glass transition,  $0.08 < \gamma_{th} < 0.43$  for these compositions for viscosities of greater than  $10^4$  Pa s.

In the case of GeO<sub>2</sub>, at the glass transition  $\gamma_{th}(T_g) \sim 0.27$ . With increasing temperature, the coefficient of thermal expansion of liquid GeO<sub>2</sub> decreases by an order of magnitude, resulting in  $\gamma_{th}(1200 \text{ }^\circ\text{C}) = 0.08$  and  $\gamma_{th}(1400 \text{ }^\circ\text{C}) = 0.007$ . This behavior is in contrast to the relatively temperature-independent behavior of the Grüneisen parameter for the melts of anorthite, diopside and albite composition over the same temperature range (Knoche et al. 1992a, b; see Table 6). The  $\gamma_{th}$  of B<sub>2</sub>O<sub>3</sub> liquid decreases from 0.20 at 400 °C to 0.02 at 1400 °C. As the Grüneisen parameter is a measure of the thermal energy in interatomic bonds in a material, this large deviation of  $\gamma_{th}$  from the “normal” (i.e.  $0.1 \leq \gamma_{th} \leq 0.4$  and relatively temperature independent) values for melts may be an indication of a coordination change occurring in these melts as a function of temperature.

### The Isochoric Heat Capacity ( $c_v$ )

The heat capacity at constant volume ( $c_v$ ) is related to  $c_p$  via

$$c_p - c_v = TV\alpha_v^2 K_T \quad (8)$$

where the symbols are the same as in [5] and [7], and  $K_T$  is the isothermal bulk modulus of the melt. The calculated value of the difference between  $c_p$  and  $c_v$  illustrates the heat capacity contribution due to  $PV$  work associated with thermal expansion. For GeO<sub>2</sub> at the glass transition temperature  $c_p - c_v = 1.3 \text{ J mol}^{-1} \text{ }^\circ\text{C}^{-1}$ . This differ-

**Table 8.**  $c_p - c_v$  for the glasses and liquids

|                               | $c_p - c_v(\text{glass})$            | $c_p - c_v(\text{liquid at } T_g)$   | $c_p - c_v(1400 \text{ }^\circ\text{C})$ |
|-------------------------------|--------------------------------------|--------------------------------------|--|
|                               | J mol <sup>-1</sup> °C <sup>-1</sup> | J mol <sup>-1</sup> °C <sup>-1</sup> | J mol <sup>-1</sup> °C <sup>-1</sup>     |
| Albite                        | 1.7–2.9                              | 4.7–7.9                              | 1.4–2.5                                  |
| Anorthite                     | 1.3–2.2                              | 4.9–8.1                              | 1.3–2.2                                  |
| Diopside                      | 2.9–4.8                              | 18.4–30.6                            | 4.5–7.6                                  |
| GeO <sub>2</sub>              | 1.2                                  | 1.3                                  | 0.002                                    |
| B <sub>2</sub> O <sub>3</sub> | 0.8                                  | 5.3                                  | 0.2                                      |

ence decreases to  $0.002 \text{ J mol}^{-1} \text{ }^\circ\text{C}^{-1}$  at 1400 °C (see Table 8). For the ternary system albite-anorthite-diopside,  $c_p - c_v$  ranges from  $1 \text{ J mol}^{-1} \text{ }^\circ\text{C}^{-1}$  in the glass, to 5–30  $\text{J mol}^{-1} \text{ }^\circ\text{C}^{-1}$  in the liquid at the glass transition, to 1–8  $\text{J mol}^{-1} \text{ }^\circ\text{C}^{-1}$  at 1400 °C (Knoche et al. 1992a, b; see Table 5). In contrast, for B<sub>2</sub>O<sub>3</sub>,  $c_p - c_v$  is  $0.8 \text{ J mol}^{-1} \text{ }^\circ\text{C}^{-1}$  for the glass,  $5.3 \text{ J mol}^{-1} \text{ }^\circ\text{C}^{-1}$  for the liquid at the glass transition temperature and  $0.2 \text{ J mol}^{-1} \text{ }^\circ\text{C}^{-1}$  at 1400 °C (Macedo and Litovitz 1965; Napolitano et al. 1965; Capps et al. 1966; Macedo et al. 1966, Gupta and Moynihan 1976; Moynihan et al. 1976; see Table 7).

### Coefficient of Volume Thermal Expansion of SiO<sub>2</sub> Melt

The geophysical parameters  $\Pi$ ,  $\gamma_{th}$  and  $c_p - c_v$  for the behavior of melts allow us to estimate the coefficient of volume thermal expansion of SiO<sub>2</sub> melt. Bacon et al. (1960) measured the thermal expansion of liquid SiO<sub>2</sub> to be  $108 \times 10^{-6} \text{ }^\circ\text{C}^{-1}$ . This value, however, is in disagreement with the value of zero, determined from the calculation of the partial molar expansivity of silicate melts (Lange and Carmichael 1990). The partial molar volume of liquid SiO<sub>2</sub> calculated from the systematic treatment of Lange and Carmichael (1990) is not in agreement with the high temperature volume data of Bacon et al. (1960) nor with the low temperature glass volume data of Brückner (1970) (see Fig. 5). Richet et al. (1982) have calculated  $\alpha_v(\text{SiO}_2)$  at 1727 °C using their own calorimetric data with the sound speed data of Bucaro and Dardy (1974) and the volume and thermal expansivity data of Bacon et al. (1960). Richet et al. (1982) obtained a value of  $-620 \text{ J mol}^{-1} \text{ }^\circ\text{C}^{-1}$  for  $c_v$  from [8], concluding that the most likely source of the error in generating this implausible result lay in the expansivity data of Bacon et al. (1960) and that a coefficient of expansivity of  $10^{-6} - 10^{-7} \text{ }^\circ\text{C}^{-1}$  (near the glassy value) produces a much more reasonable value for  $c_v$  (e.g.  $c_v > 79 \text{ J mol}^{-1} \text{ }^\circ\text{C}^{-1}$ ). This calculation, however, includes an error in the magnitude of the compressibility. A value of  $8.5 \times 10^{-13} \text{ Pa}^{-1}$  from Bucaro and Dardy (1974) is quoted, whereas the original reference reports  $\beta = 8.5 \times 10^{-11} \text{ Pa}^{-1}$ . This correct value of the liquid compressibility yields a reasonable value of  $c_v$  ( $90 \text{ J mol}^{-1} \text{ }^\circ\text{C}^{-1}$ ) via [8], with  $c_p - c_v = 5.7 \text{ J mol}^{-1} \text{ }^\circ\text{C}^{-1}$ .

The Bucaro and Dardy (1974) modulus data have been superseded by those of Krol et al. (1986). If we use the Krol et al. (1986) modulus data (12.95 GPa) and the Bacon et al. (1960) expansivity data ( $\alpha_v = 108$

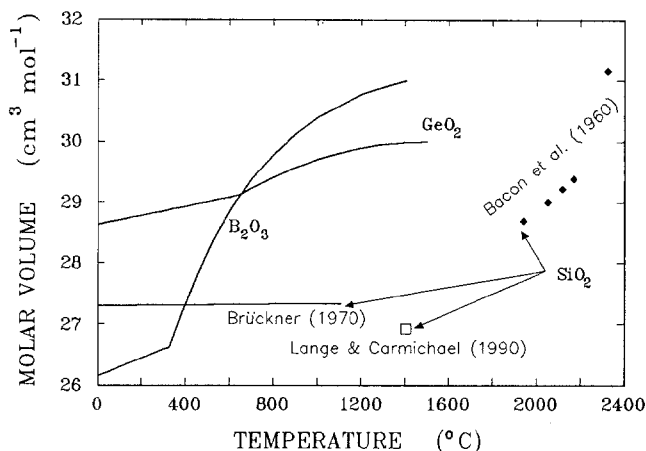


Fig. 5. The molar volume for SiO<sub>2</sub>, B<sub>2</sub>O<sub>3</sub> and GeO<sub>2</sub> glasses and liquids as a function of temperature

Table 9. Data used in the calculation of the derived parameters for SiO<sub>2</sub>

| Property  | T(°C) | liquid             | glass              | $\Phi_l - \Phi_g$ |
|---|-------|--------------------|--------------------|-------------------|
| K(GPa)  | 1100  | 12.95 <sup>a</sup> | 49.13 <sup>a</sup> |                   |
|   | 1400  | 12.95 <sup>a</sup> | 49.13 <sup>a</sup> |                   |
| $\beta(10^{-11} \text{ Pa}^{-1})$                     | 1100  | 7.72 <sup>a</sup>  | 2.04 <sup>a</sup>  | 5.69 <sup>a</sup> |
|   | 1400  | 7.72 <sup>a</sup>  | 2.04 <sup>a</sup>  | 5.69 <sup>a</sup> |
| $\alpha_v(10^{-6} \text{ }^\circ\text{C}^{-1})$       | 500   |                    |                    |                   |
|   | 1400  |                    |                    | 0.25 <sup>a</sup> |
| $c_p(\text{J mol}^{-1} \text{ }^\circ\text{C}^{-1})$  | 500   | 69.9 <sup>b</sup>  |                    |                   |
|   | 1100  | 71.6 <sup>b</sup>  |                    |                   |
|   | 1400  | 81.4 <sup>b</sup>  |                    | 8 <sup>a</sup>    |
| V(10 <sup>-6</sup> m <sup>3</sup> mol <sup>-1</sup> ) | 500   |                    |                    |                   |
|   | 1100  | 27.3 <sup>a</sup>  |                    |                   |
|   | 1400  | 27.3 <sup>a</sup>  |                    |                   |

Note: for ease of calculation, the data are presented in SI units

<sup>a</sup> Krol et al. 1986

<sup>b</sup> Richet et al. 1982

$\times 10^{-6} \text{ }^\circ\text{C}^{-1}$ ) then we obtain a  $c_p - c_v$  of  $8.25 \text{ J mol}^{-1} \text{ }^\circ\text{C}^{-1}$  for the melt at  $1400 \text{ }^\circ\text{C}$ . Although the expansivity data of Bacon et al. (1960) are relatively poorly constrained it is difficult to discard the volume data. An error of greater than 2% seems unlikely from this method.

Despite uncertainties in the input parameters for the calculation it is difficult to obtain a comparable value of  $\Pi$  for SiO<sub>2</sub> and GeO<sub>2</sub>. Krol et al. (1986) have calculated the value of the Prigogine-Defay ratio for pure SiO<sub>2</sub> to be  $2 \times 10^5$ . Their database is summarized in Table 9. They point to the uncertainty in  $\Delta c_p$  as a likely cause of the excessively high value of  $\Pi$  and argue that SiO<sub>2</sub> should have a more “normal” value of  $\Pi$  in the range of 1–10, similar to our determination for GeO<sub>2</sub>. In part this argument is based upon the similar frequency-domain mechanical relaxation behavior of SiO<sub>2</sub> and other silicate and non-silicate glasses in torsional stress experiments (Mills 1974).

The range of values determined for  $\gamma_{\text{th}}$  and  $\Pi$  representative of silicate melts can be used to estimate the

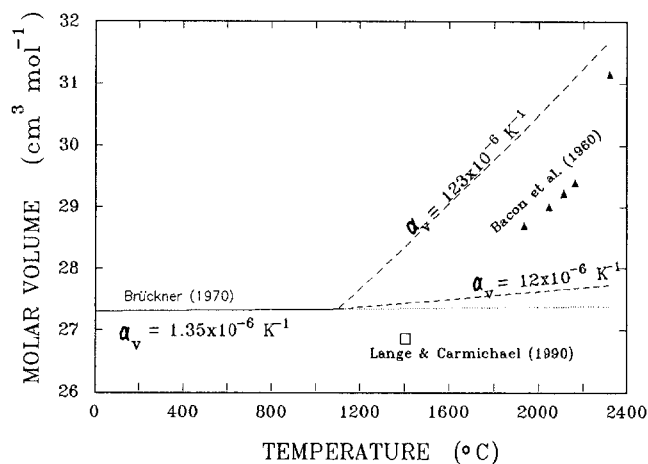


Fig. 6. Measured and calculated molar volume for SiO<sub>2</sub> glass and liquids as a function of temperature together with the estimated  $\alpha_v$  for SiO<sub>2</sub> liquid

coefficient of volume thermal expansion of SiO<sub>2</sub> melt. The “normal” range of  $\gamma_{\text{th}}$  values for silicate melts predict, at  $500 \text{ }^\circ\text{C}$ ,  $5 < \alpha_v(\text{SiO}_2) \cdot (10^{-6} \text{ }^\circ\text{C}^{-1}) < 25$  for the glass. At  $1400 \text{ }^\circ\text{C}$ ,  $23 < \alpha_v(10^{-6} \text{ }^\circ\text{C}^{-1}) < 115$  for  $0.1 < \gamma_{\text{th}} < 0.5$ . This range of  $\alpha_v$  agrees with that determined by Bacon et al. (1960) (see Fig. 6). Assuming a similar anomalous behavior of  $\gamma_{\text{th}}$  [ $\gamma(1400 \text{ }^\circ\text{C}) = 0.02$ ] for both GeO<sub>2</sub> and SiO<sub>2</sub> results in the calculation of  $\alpha_v(1400 \text{ }^\circ\text{C})$  of  $4.5 \times 10^{-6} \text{ }^\circ\text{C}^{-1}$  for SiO<sub>2</sub>. Taking  $1 < \Pi < 10$  to be representative for silicate melts, and  $1 < c_p - c_v$  ( $\text{J mol}^{-1} \text{ }^\circ\text{C}^{-1}$ )  $< 10$ , results in the calculation of  $12.3 < \alpha_v(10^{-6} \text{ }^\circ\text{C}^{-1}) < 123$  for the liquid at the glass transition.

#### $\alpha$ -SiO<sub>2</sub> vs. GeO<sub>2</sub>

It is difficult to determine the coefficient of thermal expansion of SiO<sub>2</sub> melt. There has been only one attempt to date. Bacon et al. (1960) determined the density of SiO<sub>2</sub> melt from  $1950$ – $2200 \text{ }^\circ\text{C}$  and found  $\alpha_v = 108 \times 10^{-6} \text{ }^\circ\text{C}^{-1}$ . These data have been disputed based on indirect evidence by others (Richet et al. 1982; Bottinga et al. 1983; Lange and Carmichael 1990). The argument posed by Richet et al. (1982) was based on an incorrect value of the compressibility of molten SiO<sub>2</sub>; and the coefficient of thermal expansion of Bacon et al. (1960) produces a realistic value of  $c_v$  using [8]. Thus the major theoretical objection to Bacon et al.’s data is removed. To the extent that the values of  $\Pi$  and  $\gamma_{\text{th}}$  for silicate melts presented here can be taken as representative of silicate melts in general and SiO<sub>2</sub> in particular, the thermal expansion for SiO<sub>2</sub> melt predicted from these parameters is  $12$ – $123 \times 10^{-6} \text{ }^\circ\text{C}^{-1}$ . These are “normal” expansivity values. Only anomalous values of  $\gamma_{\text{th}}$  at high temperatures as seen for GeO<sub>2</sub> and B<sub>2</sub>O<sub>3</sub> result in the calculation of small values of  $\alpha_v$ .

Thus it appears with these new data on liquid GeO<sub>2</sub> we are presented with a fundamental dilemma concerning liquid SiO<sub>2</sub>. Assumption of a liquid thermal expansivity consistent with the partial molar thermal expansivity of SiO<sub>2</sub> in silicate liquids results in values of  $\Pi$ ,  $\gamma_{\text{th}}$  and  $c_p$  that are qualitatively different to all other silicate



melts and the structural analog  $\text{GeO}_2$ . This discrepancy is despite very similar results from relaxation spectrometry on these liquids and is inconsistent with the single direct determination of  $\text{SiO}_2$  liquid density. Alternatively, a "silicate-like" value of  $\Delta\alpha_v$  at  $T_g$  that would bring all geophysical parameters into agreement and be consistent with the Bacon et al. (1960) data has eluded experimental investigations to date.

*Acknowledgements.* We thank Hubert Schulze for assistance with sample preparation.

## References

- Anderson DL (1989) *Theory of the Earth*. Blackwell, New York
- Bacon JF, Hasapis AA, Wholley JW Jr (1960) Viscosity and density of molten silica and high silica content glasses. *Phys Chem Glass* 1:90–98
- Bansal NP, Doremus RH (1986) *Handbook of Glass Properties*. Academic Press, New York
- Boehler R, Ramakrishnan J (1980) Experimental results on the pressure-dependence of the Grüneisen parameter: a review. *J Geophys Res* 85:6996–7002
- Bottinga Y, Richet P, Weill D (1983) Calculation of the density and thermal expansion coefficient of silicate liquids. *Bull Mineral* 106:129–138
- Brückner R (1970) Properties and structure of vitreous silica. I. *J Non-Cryst Solid* 5:123–175
- Bucaro JA, Dardy HD (1974) High temperature Brillouin scattering in fused quartz. *J Appl Phys* 45:5324–5329
- Capps W, Macedo PB, O'Meara B, Litovitz TA (1966) Temperature dependence of the high-frequency moduli of vitreous  $\text{B}_2\text{O}_3$ . *J Chem Phys* 45:3431–3438
- Dingwell DB, Webb SL (1989) Structural relaxation in silicate melts and non-Newtonian melt rheology in geologic processes. *Phys Chem Minerals* 16:508–516
- Dingwell DB, Webb SL (1990) Relaxation in silicate melts. *Eur J Mineral* 2:427–449
- Dingwell DB (1990) Effects of structural relaxation on cationic tracer diffusion in silicate melts. *Chem Geol* 82:209–216
- Durben DJ, Wolf GH (1991) Raman spectroscopic study of the pressure-induced coordination change in  $\text{GeO}_2$  glass. *Phys Rev* 43:2355–2363
- Gupta PK, Moynihan CT (1976) Prigogine-Defay ratio for systems with more than one order parameter. *J Chem Phys* 65:4136–4140
- Henderson GS, Fleet ME (1991) The structure of glasses along the  $\text{Na}_2\text{O}-\text{GeO}_2$  join. *J Non-Cryst Solid* 134:259–269
- Itie JP, Polian A, Calas G, Petiau J, Fontaine A, Tolentino H (1989) Pressure-induced coordination changes in crystalline and vitreous  $\text{GeO}_2$ . *Phys Rev Lett* 63:398–401
- Knoche R, Dingwell DB, Webb SL (1992a) Temperature-dependent thermal expansivities of silicate melts: the system anorthite-diopside. *Geochim Cosmochim Acta* 56:689–699
- Knoche R, Dingwell DB, Webb SL (1992b) Non-linear temperature-dependence of liquid volumes in the system albite-anorthite-diopside. *Contrib Mineral Petrol* 111:61–73
- Knoche R, Webb SL, Dingwell DB (1992c) A partial molar volume for  $\text{B}_2\text{O}_3$  in haplogranitic melt. *Can Mineral* (in press)
- Konnert JH, Karle J, Ferguson GA (1973) Crystalline ordering in silica and germania glasses. *Science* 179:177–178
- Krol DM, Lyons KB, Brawer SA, Kurkjian CR (1986) High-temperature light scattering and the glass transition in vitreous silica. *Phys Rev B* 33:4196–4202
- Kurkjian CR, Krause JT, McSimkin HJ, Andreatch P, Bateman TB (1972) In: *Amorphous Materials*, Douglas RW, Ellis B (eds). Wiley London, pp 463–473
- Lange RA, Carmichael ISE (1990) Thermodynamic properties of silicate liquids with emphasis on density, thermal expansion and compressibility. In: Nicholls J, Russell JK (eds) *Modern Methods of Igneous Petrology*. Mineral Soc Am 24:25–64
- Lesikar AV, Moynihan CT (1980) The order parameter model of liquids and glasses with applications to dielectric relaxation. *J Chem Phys* 73:1932–1939
- Macedo PB, Litovitz TA (1965) Ultrasonic viscous relaxation in molten boron trioxide. *Phys Chem Glass* 6:69–80
- Macedo PB, Capps W, Litovitz TA (1966) 2-state model for free volume of vitreous  $\text{B}_2\text{O}_3$ . *J Chem Phys* 44:3357–3364
- Mills JJ (1974) Low frequency storage and loss moduli of soda silica glasses in the transformation range. *J Non-Cryst Solid* 14:255–268
- Moynihan CT, Eastal AJ, DeBolt MA, Tucker J (1976) Dependence of the fictive temperature of glass on cooling rate. *J Am Ceram Soc* 59:12–15
- Napolitano A, Macedo PB, Hawkins EG (1965) Viscosity and density of boron trioxide. *J Am Ceram Soc* 48:613–616
- Narayanaswamy OS (1971) A model of structural relaxation in glass. *J Am Ceram Soc* 54:491–498
- Nemilov SV, Bogdanov VN, Nikonov AM, Smerdin SN, Nedbai AI, Borisov BF (1987) Values of the Prigogine-Defay relationship for inorganic glass-forming materials. *Fiz Khim Stekla* 13:801–810 (engl. trans. 1988, p 413)
- Osaka A, Takahashi K, Ariyoshi K (1985) The elastic constant and molar volume of sodium and potassium germanate glasses and the germanate anomaly. *J Non Cryst Solid* 70:243–252
- Rekhsun SM, Bulaeva AV, Mazurin OV (1971) Changes in the linear dimensions and viscosity of window glass during stabilization. *Inorg Mater (Engl Trans)* 7:622–623
- Richet P, Bottinga Y, Denielou L, Petitet JP, Tequi C (1982) Thermodynamic properties of quartz, cristobalite and amorphous  $\text{SiO}_2$ : drop calorimetry measurements between 1000 and 1800 K and a review from 0 to 2000 K. *Geochim Cosmochim Acta* 46:2639–2658
- Richet P, Bottinga Y (1986) Thermochemical properties of silicate glasses and liquids. *Rev Geophys* 24:1–25
- Richet P (1990)  $\text{GeO}_2$  vs  $\text{SiO}_2$ : glass transitions and thermodynamic properties of polymorphs. *Phys Chem Minerals* 17:79–88
- Riebling EF (1963) Structure of molten oxides. II. A density study of binary germanates containing  $\text{Li}_2\text{O}$ ,  $\text{Na}_2\text{O}$ ,  $\text{K}_2\text{O}$  and  $\text{Rb}_2\text{O}$ . *J Chem Phys* 39:3022–3030
- Rigden S, Jackson I (1991) Elasticity of germanate and silicate spinels at high pressure. *J Geophys Res* 96:9999–10006
- Rivers M, Carmichael ISE (1987) Ultrasonic studies of silicate melts. *J Geophys Res* 92:9247–9270
- Robie RA, Hemmingway BS, Fisher JR (1979) *Thermodynamic properties of minerals and related substances at 298.15 K and 1 bar ( $10^5$  Pascals) pressure and at higher temperatures*. USGS Printing Office, Washington
- Ross NL, Akaogi M, Navrotsky A, Suzaki JI, McMillan P (1986) Phase transitions among the  $\text{CaGeO}_3$  polymorphs (wollastonite, garnet, and perovskite structures): studies by high-pressure synthesis, high temperature calorimetry and vibrational spectroscopy and calculation. *J Geophys Res* 91:4685–4696
- Sasabe H, DeBolt MA, Macedo PB, Moynihan CT (1977) Structural relaxation in an alkali-lime-silicate glass. In: *Proceedings of the 11th International Congress on Glass, Prague, Vol. 1*, pp 339–348
- Scarfe CM, Mysen BO, Virgo D (1987) Pressure dependence of the viscosity of silicate melts. *Geochem Soc Spec Publ* 1:59–67
- Scherer GW (1984) Use of the Adam-Gibbs equation in the analysis of structural relaxation. *J Am Ceram Soc* 67:504–511
- Sekiya K, Morinaga K, Yanagase T (1980) Physical properties of  $\text{Na}_2\text{O}-\text{GeO}_2$  melts. *J Jpn Ceram Soc* 88:367–373
- Soga N (1969) Pressure derivatives of the elastic constants of vitreous germania at 25°, –78.5°, and –195.8° C. *J Appl Phys* 40:3382–3385
- Stacey FC (1977) *Physics of the Earth*. Wiley, New York
- Webb SL (1992) Shear, volume enthalpy, and structural relaxation in silicate melts. *Chem Geol* 96:449–457
- Webb SL, Knoche R, Dingwell DB (1992) Determination of silicate liquid thermal expansivity using dilatometry and calorimetry. *Eur J Mineral* 4:95–104